Electronic supplementary information

Synthesis of **Ru-Cu**

3-*N*,*N*-bis [(6′-methyl-2′-pyridyl)methyl]-3-aminopropyl 4′-methyl-2,2′-biphyridine-4-carboxylate (**L**)

4-Dimethylaminopyridine (102 mg, 0.84 mmol) and *N*,*N*′-dicyclohexyl carbodiimide (360 mg, 1.74 mmol) were added to the suspension of 4′-methyl-2,2′-bipyridine-4-carboxylic acid (330 mg, 1.54 mmol) in 5 ml of dry CH_2Cl_2. The resultant solution was stirred for 20 min at room temperature. A 5 ml of dry CH_2Cl_2 solution of *N*,*N*-bis[(6-methyl-2-pyridyl)methyl]hydroxypropylamine (390 mg, 1.37 mmol) was added the resultant solution, and stirred for 20 h at room temperature and then evaporated to dryness. The solid was redissolved in $CHCl_3$. The solution was applied onto a silica gel column. The product **L** was obtained as yellow oil (570 mg, 83 %). ^{1}H-NMR ($CDCl_3$, Fig.S9): *d* 2.02 (m, 2H), 2.41 (s, 3H), 2.45 (s, 6H), 2.75 (t, 2H), 4.43 (t, 2H), 6.86 (d, 2H), 7.12 (d, 1H), 7.35 (d, 2H), 7.45 (t, 2H), 7.66 (d, 1H), 8.24 (s, 1H), 8.54 (d, 1H), 8.74 (d, 1H), 8.82 (s, 1H) ppm from TMS.

$[Ru(bpy)_2(L)](PF_6)_2$ (**1**)

$[Ru(bpy)_2Cl_2]\bullet 2H_2O$ (110 mg, 0.22 mmol) and NH_4PF_6 (350 mg, 2.2 mmol) were added to the solution of **L** (110 mg, 0.22 mmol) in 5 ml of 1,2-dichloroethane. The resultant solution was refluxed for 6 h under N_2 atmosphere. The solution was filtered and the solvent was removed by evaporation. The solid was redissolved in CH_3CN, and the solution was purified by Sephadex LH-20 column chromatography using CH_3CN as eluent. After removing the solvent by evaporation, the product **1** was obtained as orange-colored oil (160 mg, 63 %). The product was stored in the dark. Just before the photochemical measurements and the preparation of **Ru-Cu** and **Ru-Zn**, the product **1** (dark red powder, 135 mg, 53 %) was refined again by recrystallization from CH_3CN/diethyl ether. ^{1}H-NMR (CD_3CN, Fig.S10): *d* 2.22(t, $2H_e$), 2.29 (s, $6H_n$), 2.42 (s, $3H_m$), 3.30 (t, $2H_d$), 4.34 (s, $4H_o$), 4.38 (t, $2H_f$), 6.91 (d, $2H_a$), 7.08 (d, 2H), 7.20 (d, $1H_j$), 7.28-7.40 (m, 4H) 7.44-7.54 (m, 4H), 7.60-7.66 (m, 4H), 7.72 (d, $1H_g$), 7.9 (m, 4H), 8.30 (s, $1H_k$), 8.40-8.47 (m, 4H), 8.62 (s, $1H_l$) ppm from TMS. $C_{49}H_{47}N_9F_{12}O_2P_2Ru_1$: calcd. C 49.67, H 4.00, N 10.64; found C 49.82, H 4.27, N 10.52.

$[Ru(bpy)_2(L)Cu(ClO_4)(H_2O)](ClO_4)(PF_6)_2 \bullet H_2O$ (**Ru-Cu**)

A CH_3CN solution (5 ml) of $Cu(ClO_4)_2\bullet 6H_2O$ (52 mg, 0.14 mmol) was added to the solution of **1** (170 mg, 0.14 mmol) in 10 ml of CH_3CN. The solution was stirred for 12 h at room tempeature in a dark place under N_2 atmosphere and then purified by Sephadex LH-20 column chromatography. A orange-colored band was collected. A brown powder of **Ru-Cu** was obtained from CH_3CN/diethyl ether (180 mg, 89 %). The product was stored in the dark. Just before the photochemical measurements, the product **Ru-Cu** was pured again by recrystallization from CH_3CN/diethyl ether. ^{1}H-NMR (CD_3CN, Fig.S11): *d* 2.06 (2H_e), 2.54 (6H_n), 2.75 (3H_m), 2.85 (br, 10H), 4.16 (2H_f), 7.25 (1H_j), 7.38 (5H), 7.55 (1H), 7.60-7.68 (7H), 7.82 (s, 1H_k), 8.04 (5H), 8.48 (7H), 8.88 (s, 1H_l) ppm from TMS. $C_{49}H_{51}N_9Cl_2Cu_1F_{12}O_{12}P_2Ru_1$: calcd. C 39.67, H 3.47, N 8.50; found C 39.79, H 3.77, N 8.67.

$[Ru(bpy)_2(L)ZnCl_2](PF_6)_2 \cdot H_2O$ (**Ru-Zn**)

To the solution of $ZnCl_2$ (142 mg, 0.10 mmol) in 80 ml of 100 mM HEPES buffer (pH 7.4), **1** (140 mg, 0.12 mmol) was added. The solution was stirred for 12 h at room tempeature in a dark place. After filtering the solution and removing the solvent by evaporation, the product **Ru-Zn** was extracted with CH_3CN from residue, and then purified by Sephadex LH-20 column chromatography using CH_3CN as eluent. A orange-colored band was collected. After removing the solvent by evaporation, a red powder of **Ru-Zn** was recrystallised from CH_2Cl_2/diethyl ether (140 mg, 80 %). ^{1}H-NMR (CD_3CN, Fig.S12): *d* 1.62 (br, 2H_e), 2.12 (br, 6H_n), 2.50 (s, 3H_m), 2.79 (br, 4H_o), 3.0 (br, 2H), 3.3 (br, 2H_d), 4.31 (br, 2H_f), 7.20 (d, 1H_j), 7.25-7.38 (5H), 7.49 (d, 1H_g), 7.63-7.73 (7H), 7.80 (2H_b), 7.96-8.05 (5H), 8.37 (s, 1H_k), 8.45 (5H), 8.75 (s, 1H_l) ppm from TMS. $C_{49}H_{49}N_9Cl_2F_{12}O_3P_2Ru_1Zn_1$: calcd. C 43.94, H 3.69, N 9.41; found C 43.65, H 3.65, N 9.57.

Figure S1 UV-visible absorption speatrum of **Ru-Cu** (solid line), $[Ru(bpy)_2(L)](PF_6)_2$ (dot line), and $[Cu(Me_2bpa)(H_2O)(ClO_4)](ClO_4)$ (broken line) in CH_2Cl_2.

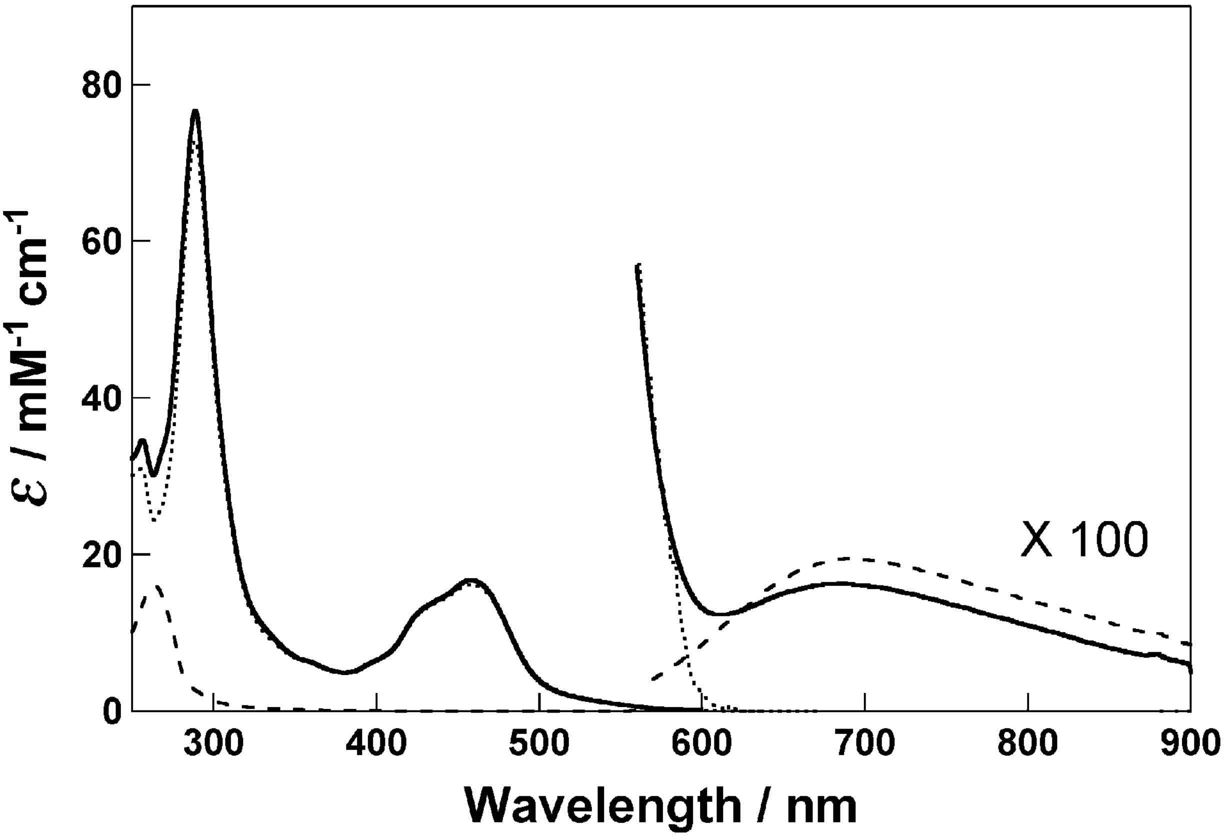

Figure S2 Emission spectra of **Ru-Cu** (solid line) and **Ru-Zn** (broken line) in acetonitrile at 25 °C. Sample concentraion is 3 mM. The excitation wavelength was 460 nm.

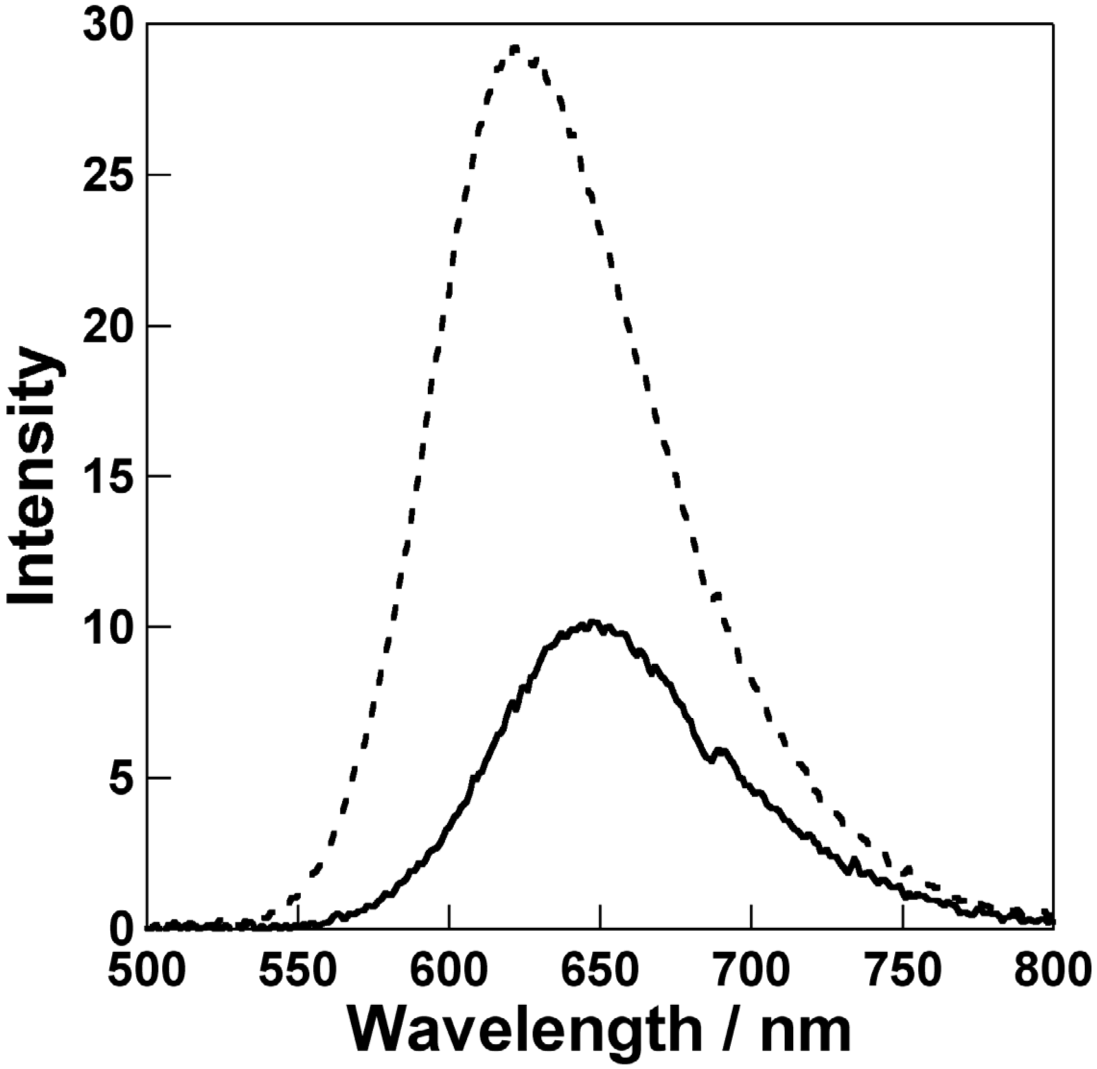

Figure S3 X band EPR spectrum of NO-Fe(DTCS)$_2$ in aqueous solution at room temperature. Instrument settings: microwave power, 1 mW and modulation width, 0.64 mT.

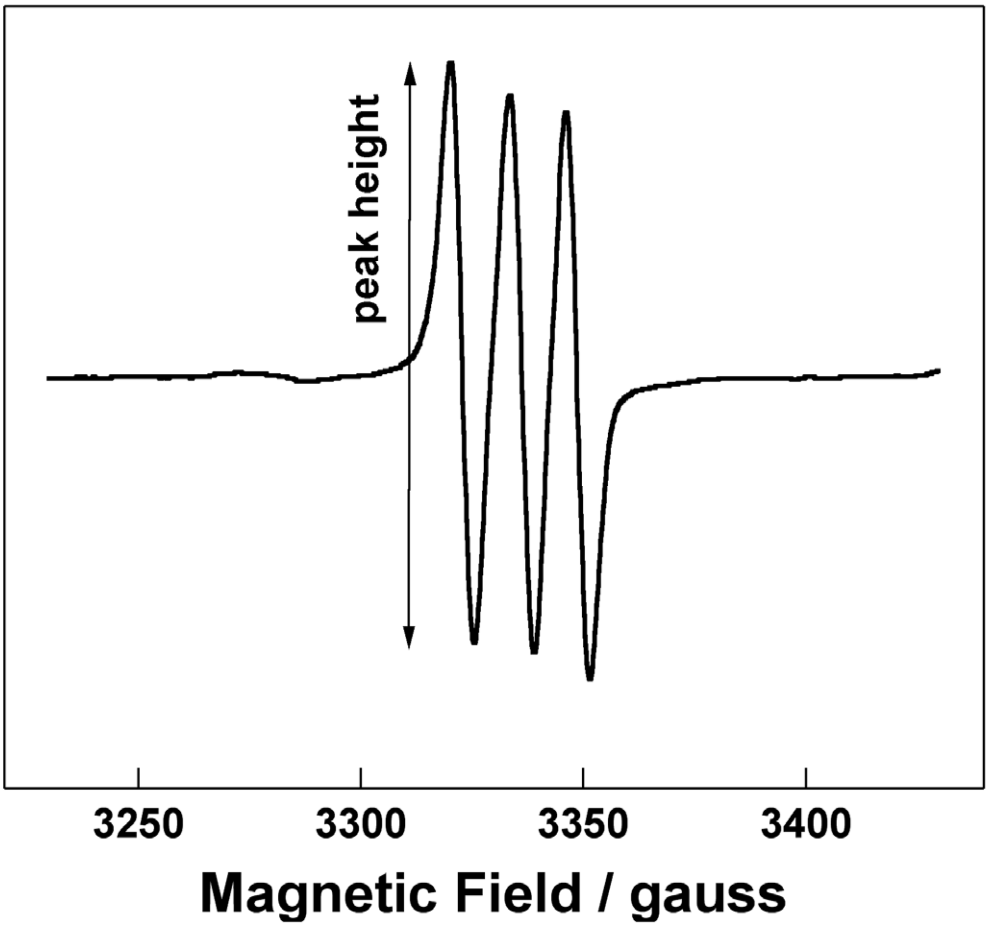

Figure S4 Plots of EPR peak-height vs. NO concentration and the calibration curve for determination of NO concentraion generated by photoreduction of nitrite.

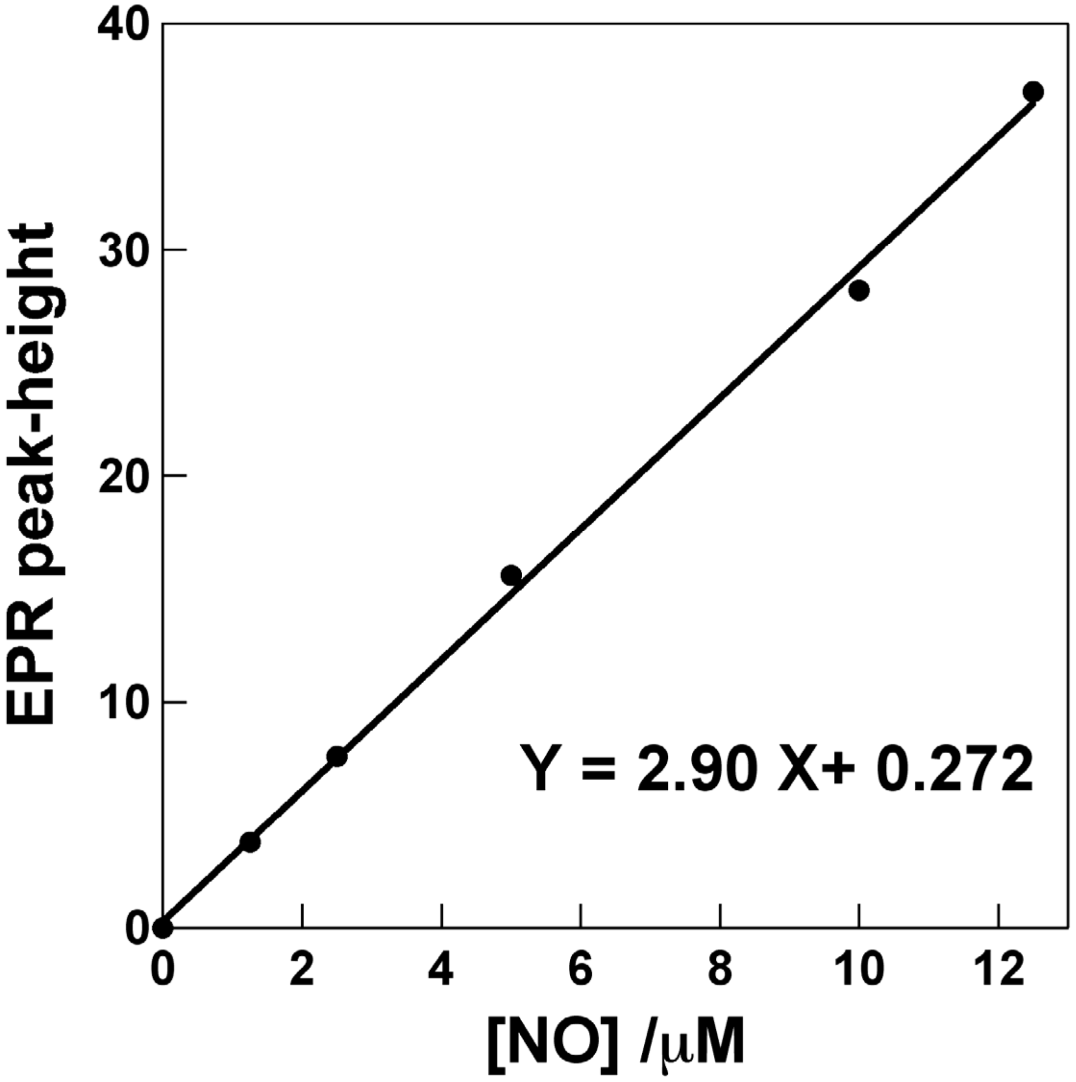

Figure S5 Transient absorption spectra after excitation of **Ru-Cu** at 532 nm (fwhm 4 ns) in deaerated CH_3CN at 298 K. Sample concentration is 60 mM. Red, 10 ns; orange, 20 ns; green, 100 ns; blue, 1 ms; and purple, 1.5 ms.

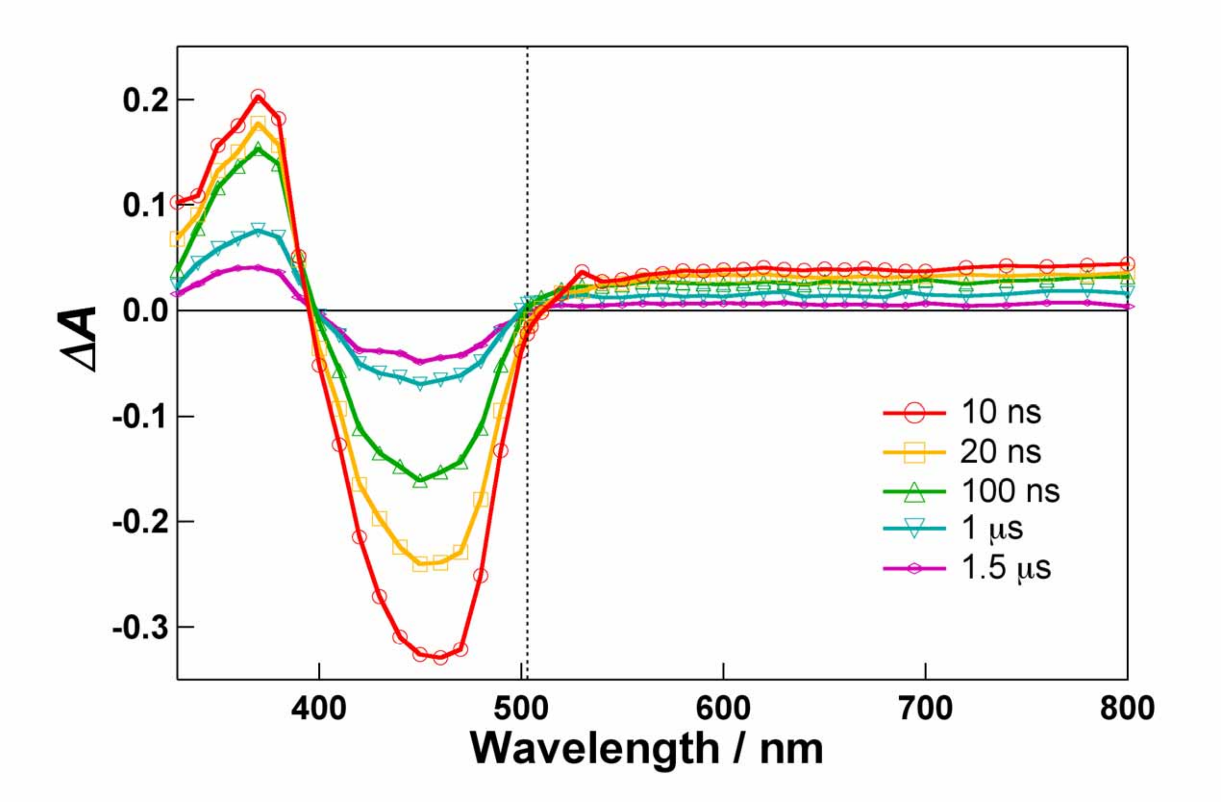

Figure S6 Transient absorption spectra after excitation of **Ru-Zn** at 532 nm (fwhm 4 ns) in deaerated CH_3CN at 298 K. Sample concentraion is 60 mM. Red, 10 ns; orange, 400 ns; green, 1 ms; blue, 2 ms; and purple, 4 ms.

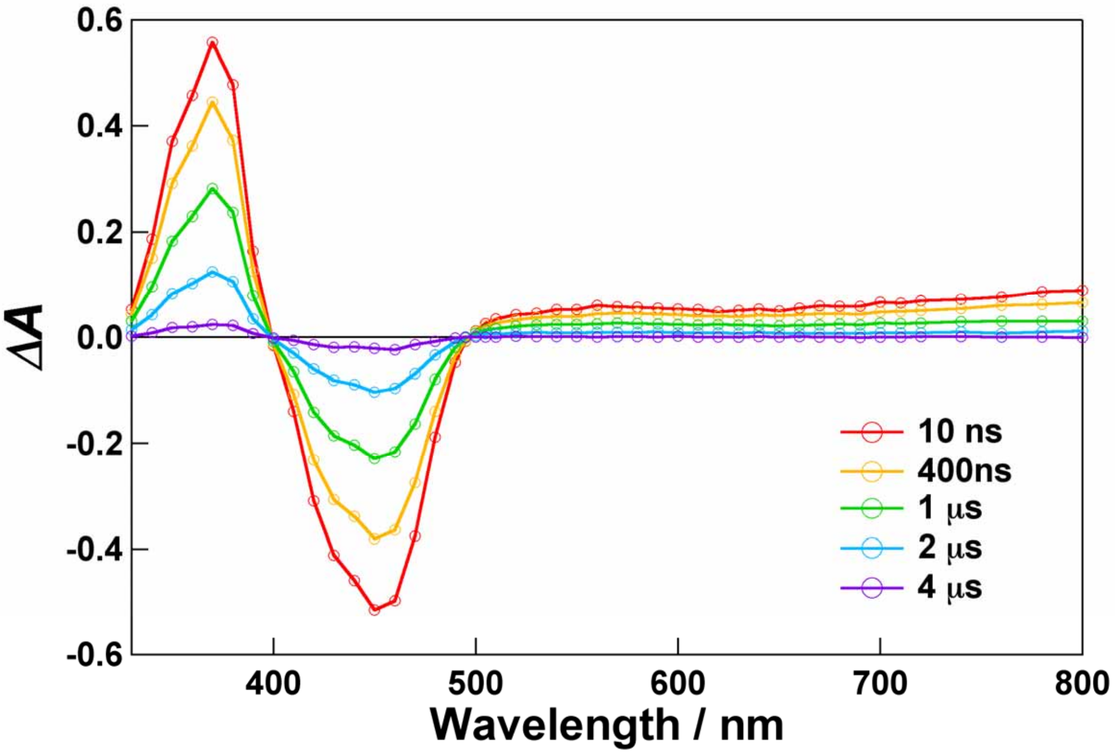

Figure S7 Time profiles of the decay of absorption at 370 nm (green line) due to the excited Ru(II) moiety and the recovery of Ru(II) ground state bleach at 460 nm (magenta line) in **Ru-Zn** at 298 K.

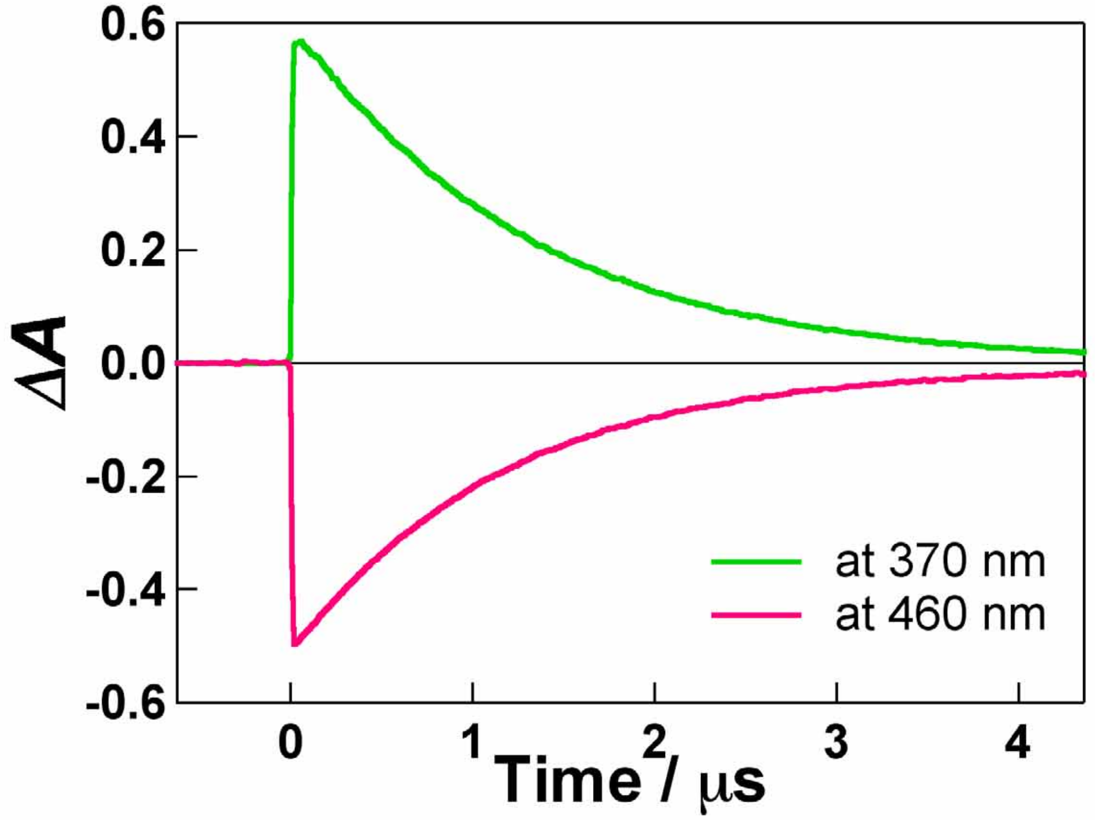

Figure S8 Time profiles of the decay of absorption at 370 nm (green line) due to the excited Ru(II) moiety, the recovery of Ru(II) ground state bleach at 460 nm (magenta line), and rise of absorbance at 503 nm due to Ru(III) (blue line) in **Ru-Cu** at 298 K.

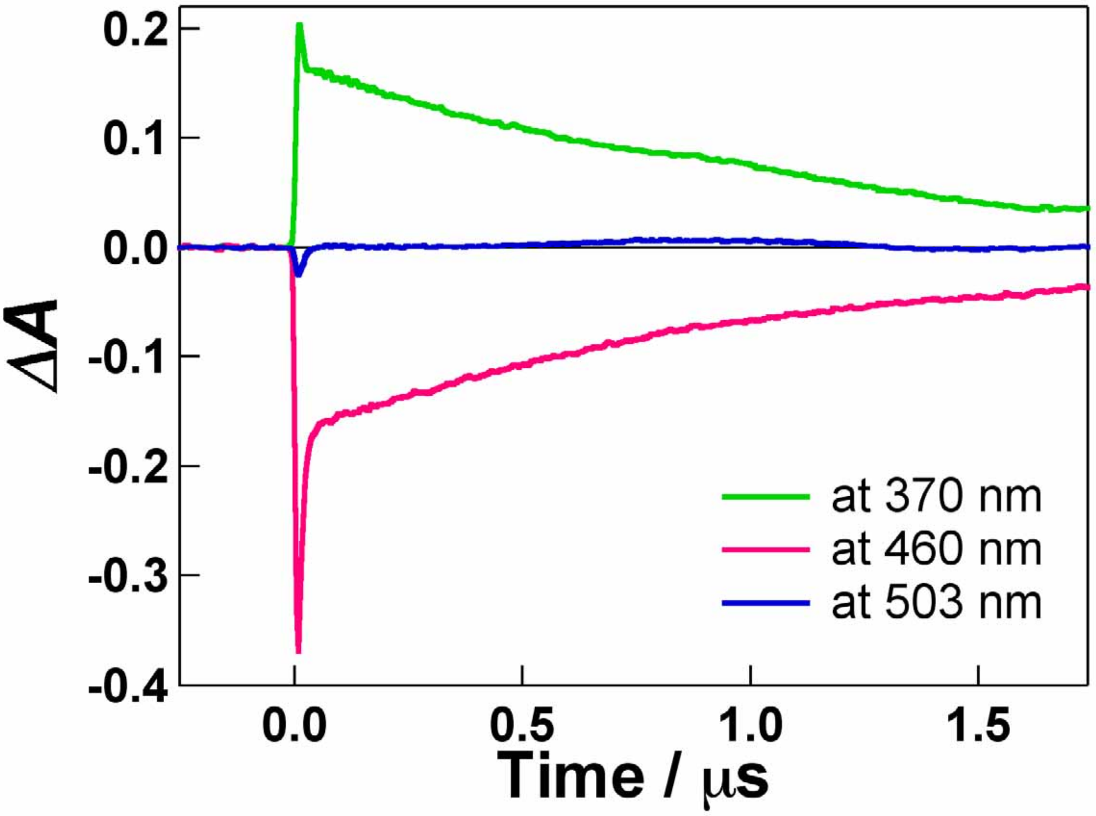

Figure S9 500MHz NMR spectrum of **L** in CDCl$_3$ at 30 °C.

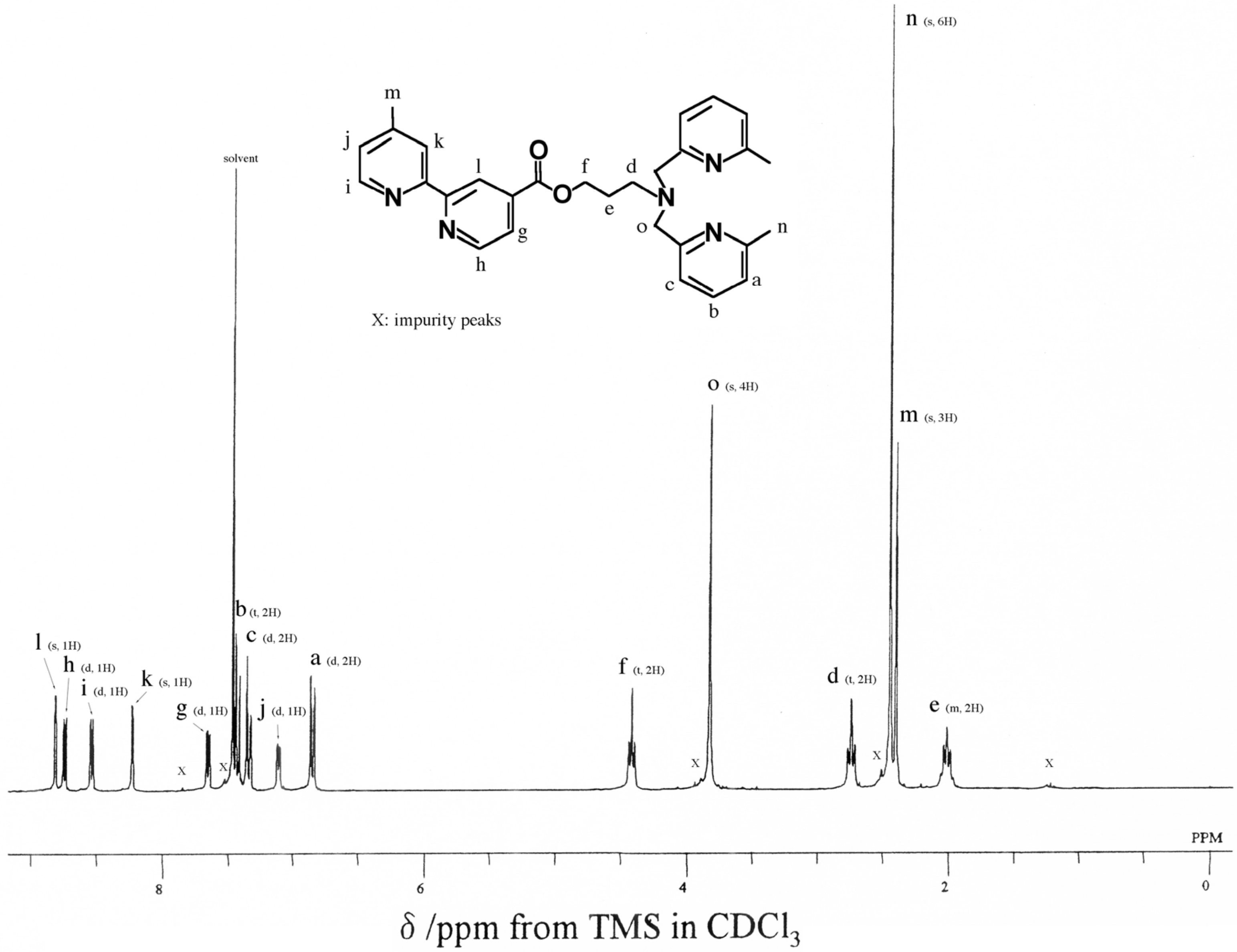

Figure S10 500MHz NMR spectrum of **1** in CD_3CN at 30 °C.

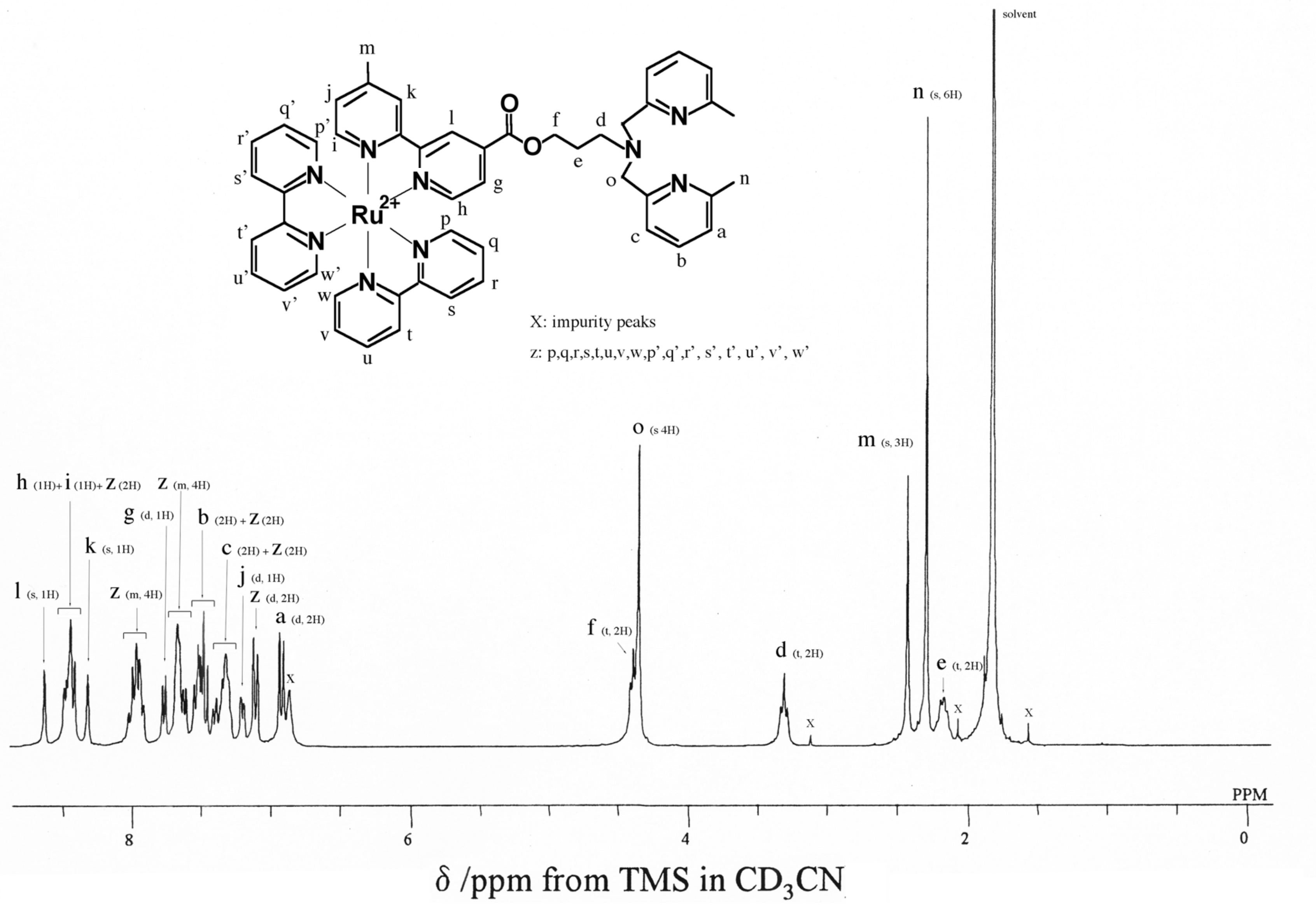

Figure S11 500MHz NMR spectrum of **Ru-Cu** in CD_3CN at 30 °C.

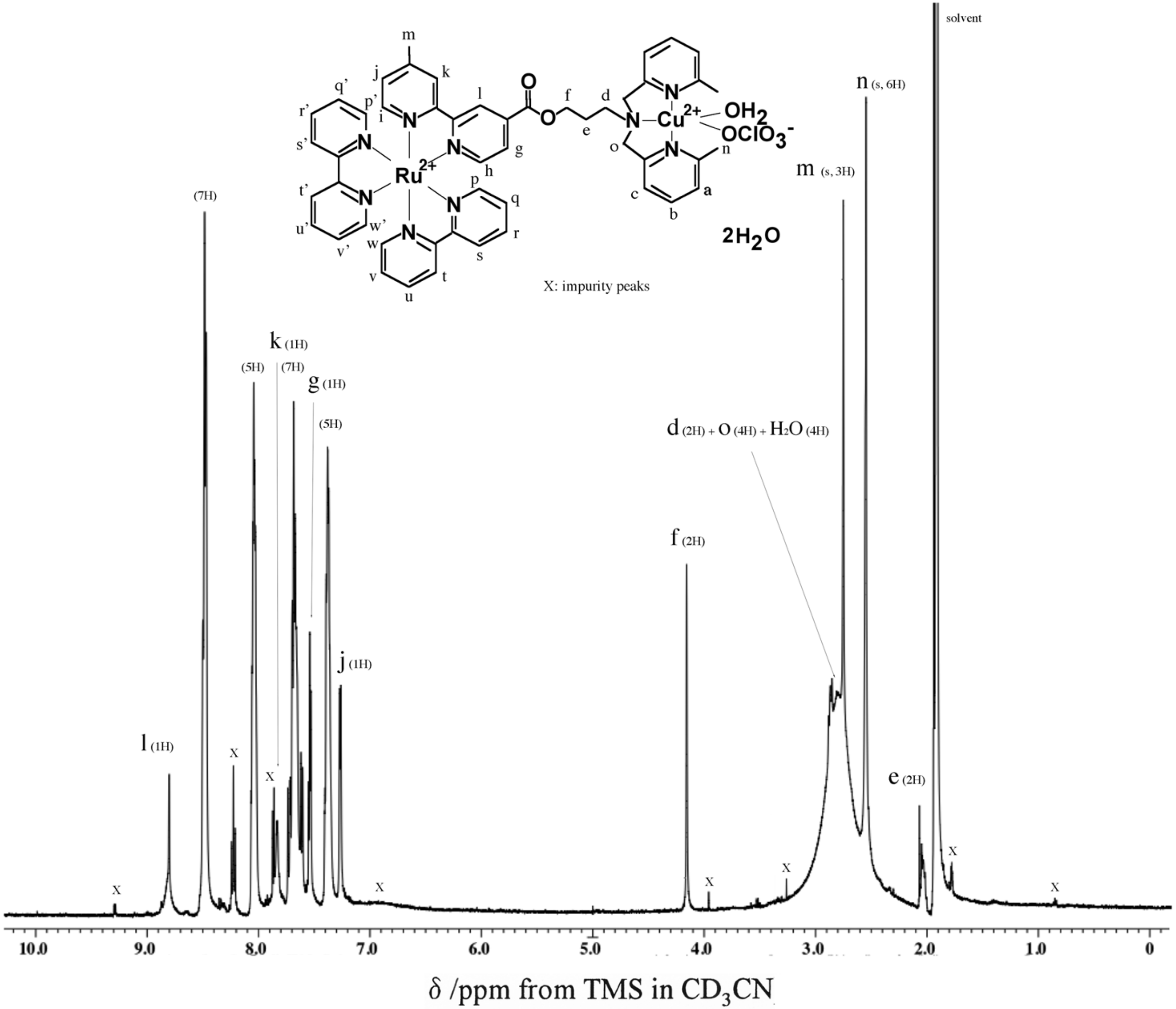

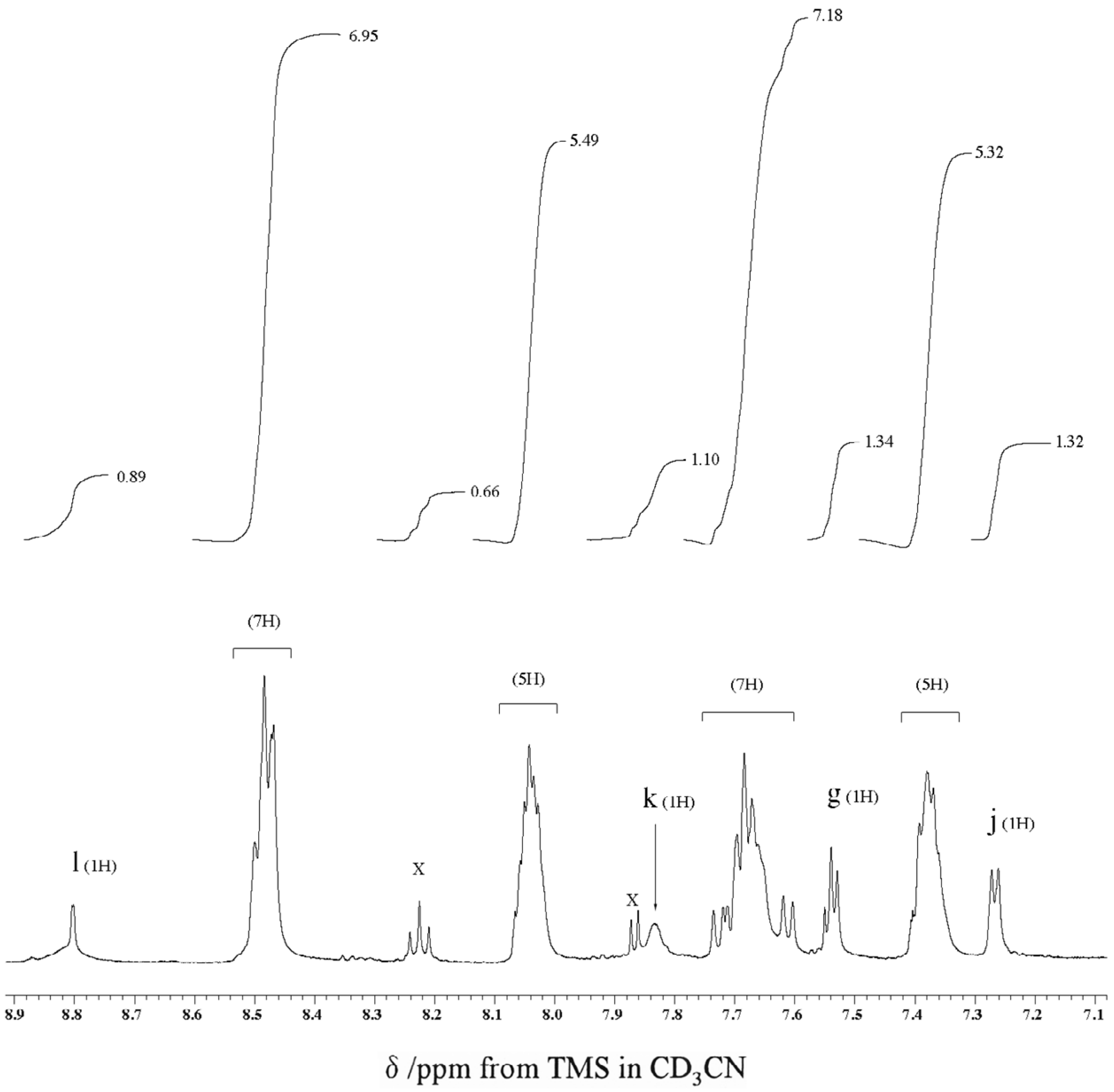
0.89
6.95
0.66
5.49
1.10
7.18
1.34
5.32
1.32
(7H)
(5H)
(7H)
(5H)
l (1H)
x
x
k (1H)
g (1H)
j (1H)
8.9
8.8
8.7
8.6
8.5
8.4
8.3
8.2
8.1
8.0
7.9
7.8
7.7
7.6
7.5
7.4
7.3
7.2
7.1
δ /ppm from TMS in CD_3CN

Figure S12 500MHz NMR spectrum of **Ru-Zn** in CD_3CN at 30 °C.

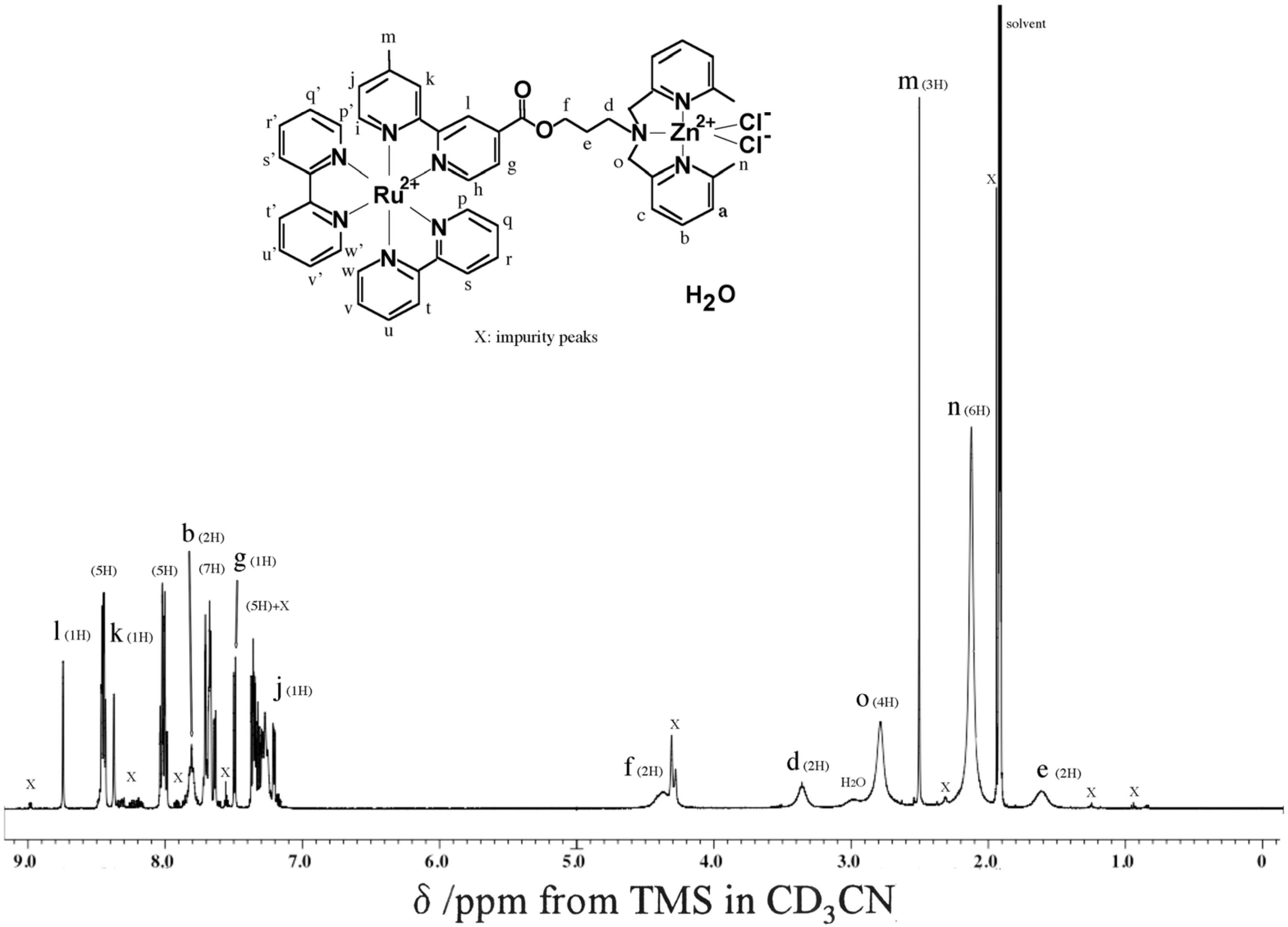

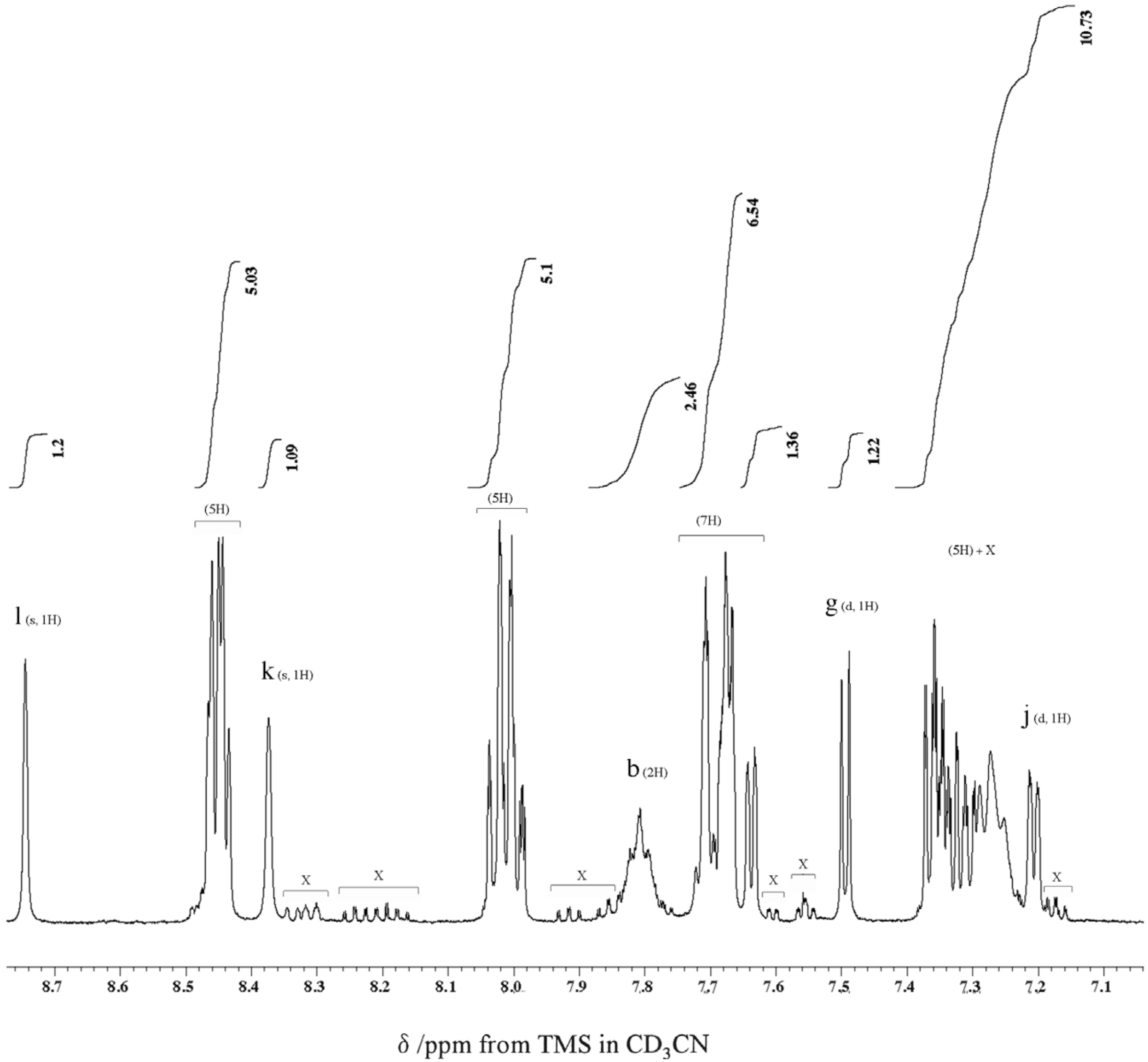
1.2
5.03
1.09
5.1
2.46
6.54
1.36
1.22
10.73
(5H)
(5H)
(7H)
(5H) + X
l (s, 1H)
k (s, 1H)
b (2H)
g (d, 1H)
j (d, 1H)
X
X
X
X
X
X
X
8.7
8.6
8.5
8.4
8.3
8.2
8.1
8.0
7.9
7.8
7.7
7.6
7.5
7.4
7.3
7.2
7.1
δ /ppm from TMS in CD_3CN

Effect of minor impurity on the observed reactivity of Ru-Cu complex

As some peaks of impurities were observed in NIR spectra (Figures S9-12), the **Ru-Cu** sample was is not 100% pure perfectly. In order to investigate the effect of minor impurity for the observed reactivity of **Ru-Cu**, we tried to get the single crystal of Ru-Cu complex and pure Ru-Ru dimmer as a candidate for the impurity material. In our experiments, Ru-Cu complex is the racemic compound of two chiral Ru-Cu complexes. The mixture of chirality in Ru-Cu might be one of the disturbance for single-crystallization, although there are not any evidence. We carried out an alterative experiment to check the effect of impurities. The photoreduction experiment of "the candidate for Rubpy$_3$-RuMe$_2$bpy complex", which is obtained from the reaction of **L** and 3 equiv. of Ru(bpy)$_2$Cl$_2$, was conducted. However, any NO-generation was not observed under the same experimental condition as our manuscript. Accordingly, Ru-Ru dimmer should have no reactivity. I suppose that the possibility of Ru-Ru dimer as an impurity of Ru-Cu sample could be low, because the synthesis steps for Ru-Cu are as follows.

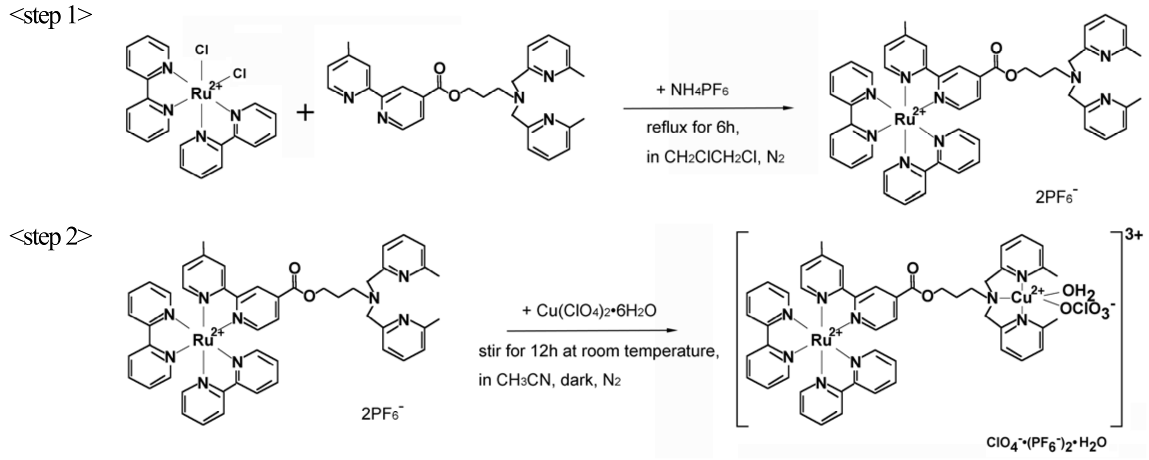

On the second step, the reaction was carried out at room temperature. For making Ru-Ru dimer, the bond between Ru ion and N ligand of bpy must be broken and the free Ru ions must bound to bpa ligand instead of Cu ions. We can not believe the reaction would be occurred at the temperature, The first step is usual method for synthesis of Ru(bpy)$_3$ from Ru(bpy)$_2$Cl$_2$. We separated the [Ru(bpy)$_2$(L)](PF$_6$)$_2$ complex from byproducts and starting materials by column chromatography. If the sample included the reactive impurity, the photoreduction of nitrite by the sample would be observed. Although we have checked the reactivity of [Ru(bpy)$_2$(L)](PF$_6$)$_2$ sample, the NO formation did not occur.

Effect of solvent on laser flash photolysis experiments

We have tried the laser flash photolysis of Ru-Cu in CH$_2$Cl$_2$ at first. However, we were not able to get the clear results. The absorbance of Ru-Cu was not thoroughly recovered after laser flash in CH$_2$Cl$_2$. The Ru-Cu complex would be broken in CH$_2$Cl$_2$ under high-power light. In other words, the excited Ru-Cu complexes (Ru^{2+}*–Cu^{2+}, Ru^{3+}–Cu^{2+} or Ru^{3+}–Cu^{1+}) could react with CH$_2$Cl$_2$. In MeCN, however, we can get the good results of laser flash photolysis as shown in the main text. Accordingly, the Ru-Cu complex is stable in MeCN under high-power light. Therefore, we carried out the photoreaction experiments in MeCN and the generation of products was not observed in MeCN in the absence of sacricial reductant as mention in the main text.

Consideration of the reason that the reaction stop after NO generation equivalent to 10% of the dinuclear complex

One possibility is that the **Ru-Cu** might be broken even under lower-power light than laser, although the UV-vis spectrum of **Ru-Cu** after the reaction is almost the same as that before the reaction. Another possibility is that the generated NO might react with **Ru-Cu**. Or the some radicals (for example: Cl$^•$) might prevent the photoreduction of nitrite or react with NO. However, we cannot state the speculation in this manuscript because we have no solid evidence so far.